

# Novel Glucose Oxidase Interlocked Prussian Blue/Polysulfone Stereo-Structure and its Application in Amperometric Glucose Biosensor

Cang Wang<sup>1</sup>, Min Pan<sup>1</sup>, Hang Chen<sup>1</sup>, Dajing Chen<sup>2,\*</sup>, Yuquan Chen<sup>1,\*</sup>

<sup>1</sup> Department of Biomedical Engineering, Zhejiang University, Hangzhou 310027, China

<sup>2</sup> Medical School, Hangzhou Normal University, Hangzhou, 311121, China

\*E-mail: [djchen@hznu.edu.cn](mailto:djchen@hznu.edu.cn)

Received: 25 March 2019 / Accepted: 21 May 2019 / Published: 30 June 2019

---

In this study, we present a controllable Prussian Blue (PB)- Polysulfone (PSF) stereo-structure with glucose oxidase (GOD) interlocked for glucose biosensing. This work links the electrochemical catalytic properties of PB with the large surface area and mass transport of three-dimensional macro-porous PSF and highlights the importance of interlocking GOD with PB to improve sensor sensitivity and linearity, which also maintains glucose sensor activity. The prepared PB-PSF-GOD glucose biosensor exhibited a 1-12 mM linear range, high affinity and good selectivity with a low applied potential of -0.05 V (vs Ag/AgCl). Furthermore, the prepared sensor only attenuated by 10% after 7 days of continuous testing. The advanced properties of the novel GOD interlocked PB-PSF structure may have promising applications in enzymatic biosensors, especially the continuous glucose monitoring (CGM).

---

**Keywords:** Prussian blue; nanostructure; glucose oxidase; glucose biosensor; nanocoating

## 1. INTRODUCTION

Blood glucose monitoring is critically important and urgently needed for the management of both type I and type II diabetes. Through precise glucose concentration detection throughout the day and night, the adverse effects caused by type II diabetes mellitus can be effectively controlled through Continuous Glucose Monitoring (CGM) with insulin injections or pills (i.e., sulphonyl urea)[1, 2]. Glucose levels in diabetic patients vary from 2 mM to 40 mM[3], and there is a considerable need for the development of highly reliable, wide-linear-range and long-life glucose biosensors[4, 5]. Due to the great selectivity and ease of testing, GOD-based biosensors are one of the most widely used glucose biosensors among all kinds of promising glucose biosensors, especially as CGM sensor[6, 7].

PB, which is a typical hexacyanoferrate coordination compound, is a highly efficient electrode modifier for GOD-based glucose biosensors[8]. It has a stable cubic cell structure and is composed of the following three elements: iron, carbon and nitrogen[9], which make PB a simple metal organic framework (MOF). Similar to other MOFs, PB has exhibited many catalytic properties, such as a tunable cell-structure size, a highly specific surface area and abundant surface functional groups. As previous studies have reported, PB-applied biosensors are able to sense hydrogen peroxide at a low applied potential, which makes PB an “artificial peroxidase” analogous to peroxidase enzymes for hydrogen peroxide reduction[10]. In addition to its catalytic function, PB is also well-known for its nontoxicity and biocompatibility[11]. Due to the above characteristics, PB is widely employed with GOD for glucose biosensors[12].

Together with the development of nanotechnology, porous PB nanostructures are widely adopted in glucose biosensors, taking the place of crystalline powder samples as electrochemical mediators[13-16]. The porous stereo-structures in PB mixtures that link the functional interfaces and nano-PB particles are in a rapidly developing field[10]. Various assembly strategies have been studied for nano-PB-integrated stereo-structures, including direct electrodeposition[17], seed-mediated growth[18], molecular 3D imprinting[19], “electroless” deposition[20] and spontaneous self-assembling. However, most researchers focus on nano-PB itself, ignoring the interactions between nano-PB and substrates. Due to the cooperation between nano-PB and substrates, the sensor as a whole will undergo interesting changes. In particular, substrate materials with special structures are especially worthy of concern. Additionally, the porous structures in flexible substrates are always fragile and the life of the sensor is rarely mentioned[10, 20-22].

In the present work, we report a novel PB-PSF stereo-structure with interlocked glucose oxidase (PB-PSF-GOD) and explore its application as an amperometric glucose biosensor. In contrast to traditional PB deposition, the fabricated PB layer maintains the 3D structure of the PSF substrate and thoroughly covers the inner surface of the substrate with GOD interlocked in the hydrophilic-modified PSF membranes under mild reaction conditions. Additionally, flexible amperometric glucose biosensors based on the PB-PSF-GOD were developed with a great linear range, good selectivity and long life. The results demonstrated that PB-PSF-GOD structures with potential features could be a promising platform for enzymatic biosensors, especially the CGM.

## 2. EXPERIMENTAL

### 2.1 Reagents and apparatus

All chemicals used were of analytical grade and were used as received without any further purification. Modified PSF porous membranes were obtained from Harvest company as commercial products. The carbon slurry was purchased from the Acheson colloids company (Product: Electrodag 423SS). Glucose oxidase (EC 232-601-0, from *Aspergillus niger*) and Bovine serum albumin (BSA) were purchased from Aladdin. Glucose, glutaraldehyde (GA), uric acid (UA), ascorbic acid (AA), hydrochloric acid (HCl), potassium chloride (KCl), ferric chloride ( $\text{FeCl}_3$ ), potassium ferricyanide ( $\text{K}_3\text{Fe}(\text{CN})_6$ ), paraffin wax, Sodium phosphate ( $\text{Na}_2\text{HPO}_4$ ), sodium dihydrogen phosphate ( $\text{NaH}_2\text{PO}_4$ ),

sodium hydroxide (NaOH), hydrogen peroxide (H<sub>2</sub>O<sub>2</sub>) and ProClin 300 were supplied by Sigma-Aldrich (China). The supporting electrolyte used for the electrochemical studies was 0.05 M phosphate buffer solution (PBS), prepared using Na<sub>2</sub>HPO<sub>4</sub> and NaH<sub>2</sub>PO<sub>4</sub> and the pH was adjusted either using HCl or NaOH. Glucose solution was stored at 26°C for 24 h for mutarotation before use. Aqueous solutions were prepared in deionized water (DI). Fresh blood samples were provided from three healthy volunteers and two diabetes patients.

The peristaltic pump used for the bubbling solution was a BT00-100M from the Igpump company. The morphologies of the PSF and PB deposition were studied using a Hitachi SU8010 field-emission scanning electron microscope (SEM). Fourier transform infrared (FT-IR) spectra were recorded with an AVATAR 370 in reflectance mode. All electrochemical measurements were performed on a CHI 660A electrochemical workstation (Shanghai Chenhua, China). A standard three-electrode system was used for all electrochemical experiments, with an Ag/AgCl (1.0 M KCl) electrode and a platinum net (geometric area, 0.96 cm<sup>2</sup>) as the reference and counter electrode, respectively. PBS (0.1M pH=5) was used as the supporting electrolyte for electrochemical tests. Cyclic voltammetric (CV) curves were obtained at 50mVs<sup>-1</sup> and electrochemical impedance spectroscopy (EIS) were carried out at frequency of 1Hz to 10<sup>5</sup> Hz. Amperometric detection was operated at applied potential of -0.05V. The serum glucose analyses were conducted using a YSI 2300 STAT PLUS (Yellow Springs Instruments, Ohio, USA). All of the experiments were conducted at room temperature.

## 2.2 Immobilization of GOD on modified porous PSF membranes

Before the immobilization of GOD, uniform-cut hydrophilic porous PSF membranes (geometric area, 0.30 cm<sup>2</sup>) were washed by immersing in deionized water for 24 h and dried overnight at room temperature. The GOD solution was freshly prepared by dissolving 15 mg GOD and 8 mg BSA (for GOD protection) in 1 ml deionized water. To immobilize GOD on the modified PSF membrane (Scheme, Fig. 1), an appropriate amount of GOD solution (2 μL) was evenly dropped on top of the modified PSF membrane and dried by sticking absorbing paper on the other side for 1 min. Then, 2 μL of 5% GA solution (for crosslinking) was dropped and dried in the same way. After drying under air at room temperature for 30 min, the resulting membrane was rinsed 3 times with deionized water and dried in drying oven at 40°C for preparation.

## 2.3 Synthesis of PB

For the synthesis of PB, a PB self-assembling reaction was carried out (Scheme, Fig. 1) as follows. (i) Prepared membranes were soaked in 0.01 M K<sub>3</sub>Fe(CN)<sub>6</sub> (pH = 4, adjusted by HCl) solution and bubbled with a peristaltic pump (100 rpm) for 1 min, before being dried with absorbing paper stuck to the bottom surface for 15 min at room temperature. (ii) The K<sub>3</sub>Fe(CN)<sub>6</sub>-treated membrane was gradually immersed into 0.02 M FeCl<sub>3</sub> and 0.1 M glucose solution mixture (1:1), then bubbled with the peristaltic pump (100 rpm) for 5 min. During this process, the color of the membrane changed gradually from light yellow to blue. (iii) After bubbling, the membrane was carefully washed 3-4 times with

deionized water and dried in a drying oven at 40°C for 1 h. To cover the PB on GOD interlocked PSF membrane (Scheme, Fig. 1), this procedure was repeated 15, 30 and 45 times, followed by FTIR spectroscopy.

### 2.4 Preparation of the modified biosensor

To prepare easily fabricated, flexible amperometric glucose biosensor, an appropriate amount of carbon slurry was brushed on the bottom surface of the membrane.

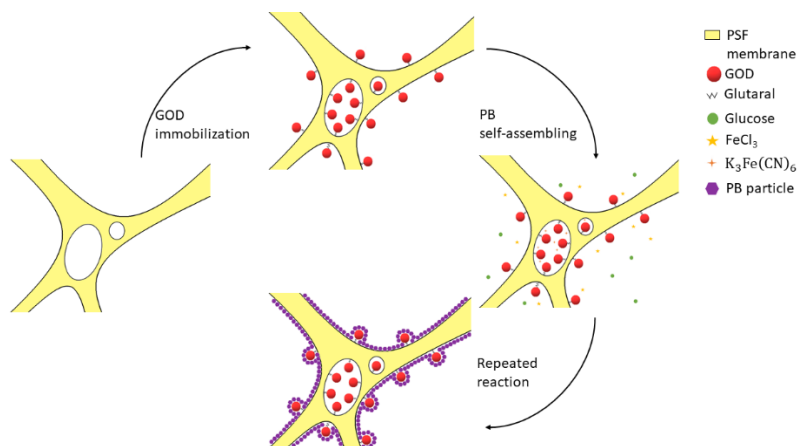


**Figure 1.** Schematic for the fabrication of Prussian Blue covered GOD-interlocked porous PSF membranes.

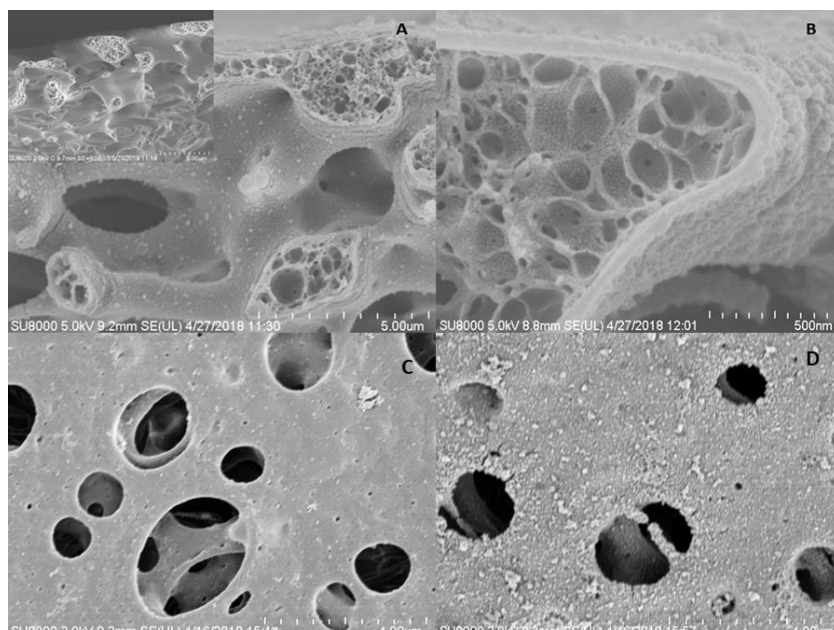


**Figure 2.** (a) SEM image of modified porous PSF membrane (upper left) and the PB covered PSF membrane cross-section. (b) An enlarged image of the PB covered GOD interlocked porous PSF film cross-section. (C) Image of modified porous PSF membrane (D) Image of PB covered GOD interlocked porous PSF

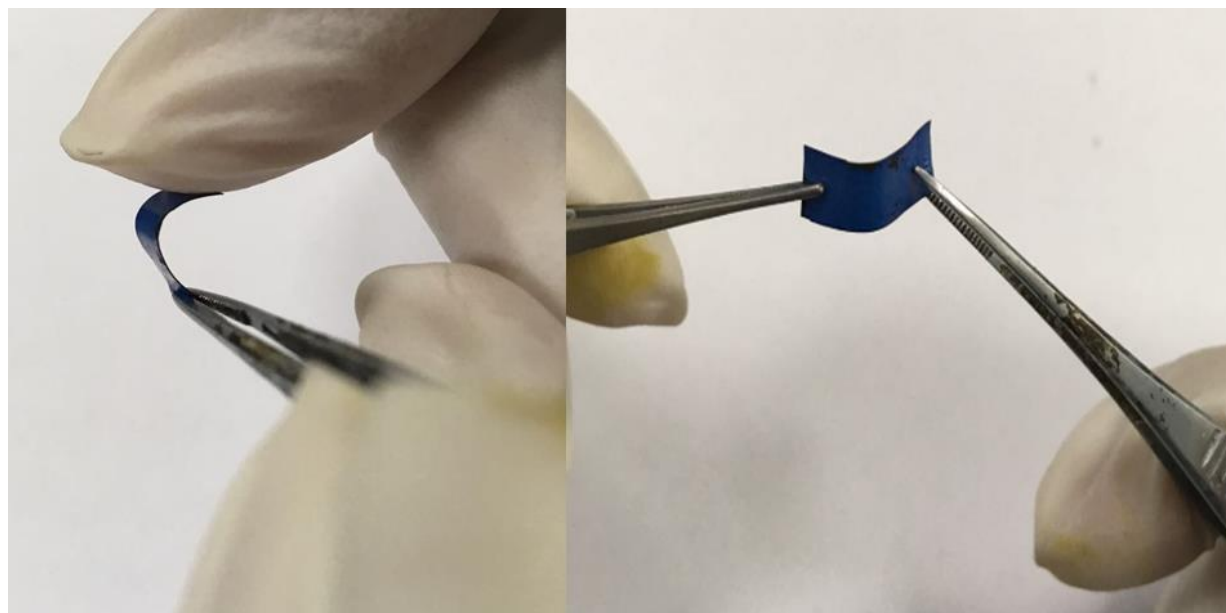


**Figure 3.** PB covered porous PSF membrane flexibility (with 15 cycles PB synthesis procedure).

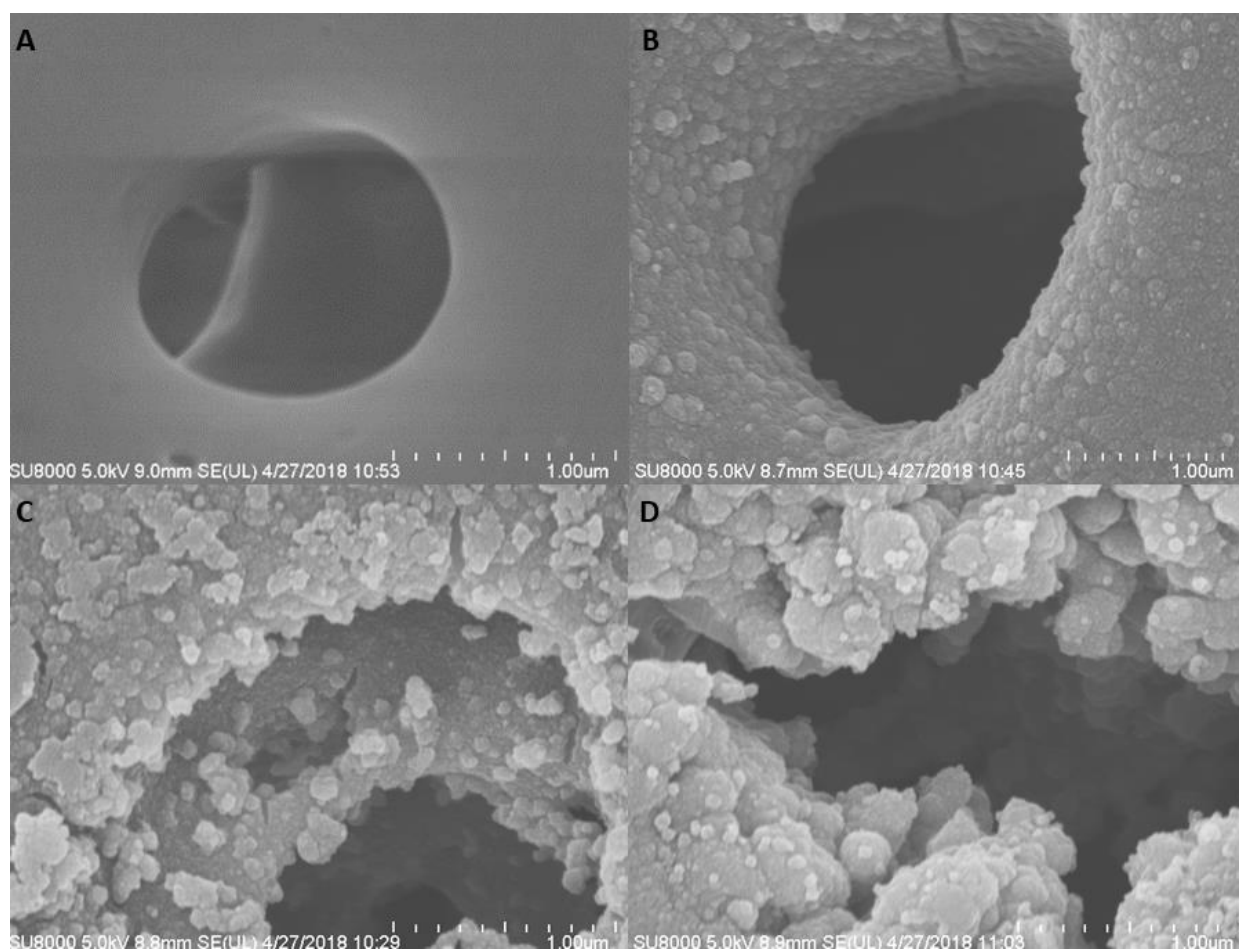


**Figure 4.** SEM images of PB layer morphologies formed by the procedure repeated (a) 0 times, (b) 15 times, (c) 30 times and (d) 45 times

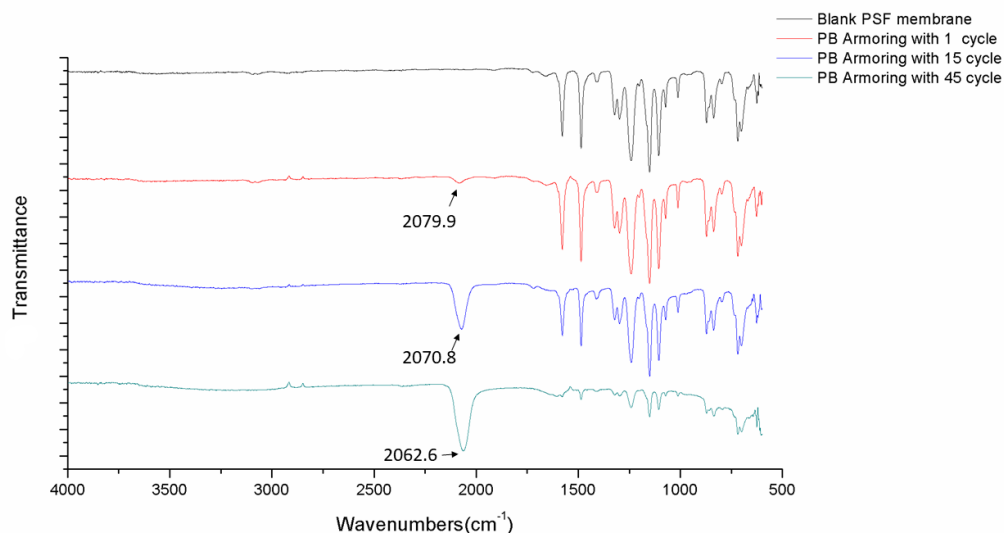


**Figure 5.** FT-IR spectra of the PB formed the procedure being repeated (a) 0 times, (b) 15 times, (c) 30 times and (d) 45 times.

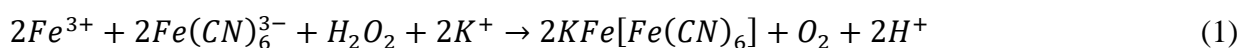
After drying overnight in a fume hood at room temperature, paraffin was coated on the bottom to prevent direct contacts between the carbon slurry and the solution. Part of the sensor was protected by plastic plate, leaving a 1 mm diameter hole in contact with the solution. The biosensor was stored in the fridge at 4°C when not in use. The modified PB-PSF-GOD biosensor maintains great flexibility in the presence of the pasted carbon slurry and wax.

### 3. RESULTS AND DISCUSSION

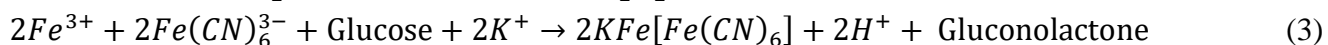
#### 3.1 Preparation of PSF-GOD and PB-PSF-GOD

Previously, PEDOT or graphite foam [14, 20] with three dimensional macroporous structure was used as the matrix to grow PB nanoparticles. Here, another important polymer PSF was used to support PB. Fig. 2a, c, d and Fig. 4a show the SEM images of the modified PSF film. The low magnified image shows the PSF film has a network type morphology with micron-sized pores (Fig. 2c). Highly magnified image indicates these macropores are interconnected, which could facilitate mass transport [19, 20, 23] and provides a large surface area for reaction and enzyme immobilization. Moreover, lots of fiber-like structures and extruded tubular structures cross-linked with each other in the PSF film (Fig. 2a, up-left), which could provide great active sites for GOD bonding.

Next, Nano-PB particles were formed on this PSF matrix through a spontaneous reaction between  $\text{FeCl}_3$  and  $\text{K}_3\text{Fe}(\text{CN})_6$  in the presence of a slight excess of  $\text{H}_2\text{O}_2$ , as Liu [24] published, due to the high open potential (+1.22 V) in the  $\text{Fe}^{\text{III}} - \text{Fe}^{\text{III}}(\text{CN})_6$  state [25]. The PB formation reaction can be expressed as follows:



Here, instead of directly mixing [24],  $H_2O_2$  was gradually generated in a reaction with glucose and immobilized GOD (Formula 2), which is trapped in PSF flexible membrane and protected by the GA and BSA composite. The formation can be described as Formula 3.



Combine the SEM and subsequent electrochemical results (Fig. 2a,b,d and Fig. 5), a layer of well dispersed PB particles uniformly anchor on the PSF membrane instead of traditional PB bulk deposition[8, 14, 21, 26]. The average size of these particles is about 100nm. During preparation, the entrapped GOD may have three functions. First, GOD as a glucose-sensitive agent produce  $H_2O_2$  to initiate the spontaneous growth of PB. To demonstrate the active role of the GOD, experiment revealed that almost no PB was generated on PSF within 30 min if immersing just BSA interlocked PSF film in the growth solution of PB. Second, the GOD provides insufficient nuclei for the crystallization process to generate PB particles with small size and improved dispersity. This may be explained with the nonclassical seed-mediated growth theory[27]. First, quantities of low solubility Prussian blue nuclei were formed in the closest place to the interlocked GOD. Once a new particle is nucleated, the hydrogen peroxide gradient drives it to the gap between two particles with glucose as nanocrystallite stabilizer[18]. This was confirmed by the facts that spherical PB with aggregation was formed on PSF film if the glucose concentration in PB precursor solution increased from 0.1M to 1M (Fig. S1), and the flocculation was formed as soon as  $H_2O_2$  added into the precursor solution. Third, the GOD provides great selectivity and sensitivity in prepared glucose sensor (Fig. 7,8).

### 3.2 Effects of reaction cycles on PB generation

To optimize the formation of the PB layer, the membranes were produced with different reaction cycles (ranging from 0 to 45). As shown in Fig. 4, obvious PB deposition grows as the number of reaction cycles increases. At 45 cycles, the original PSF macropores were blocked with stacking PB deposition, which is likely attributed to the excess crystallization speed for seed formation on the inner surface of the pores[8]. The FT-IR spectra of the PB layer morphologies formed by various cycles were illustrated in Fig. 5. These results further confirmed that the PB nanoparticles successfully covered the porous PSF membrane. In the FT-IR spectrum of PB layer forming with 1 cycle, a new sharp absorption peak appeared at  $2079.9 \text{ cm}^{-1}$  on the PB covered PSF surface compared with the original PSF surface. This peak corresponded to the CN stretching absorption band of the PB  $Fe^{2+}$ -CN- $Fe^{3+}$  CN group[28]. Additionally, there was no peak at  $2168 \text{ cm}^{-1}$ , which was characteristic of a Berlin green  $Fe^{2+}$ -CN- $Fe^{3+}$  bond[29], revealing that no Berlin green (which has a similar structure to PB) was formed on the surface of the electrode. The peaks at  $2070.8 \text{ cm}^{-1}$  and  $2062.6 \text{ cm}^{-1}$ , which correspond to PB layer forming with 15 and 45 cycles, respectively, are characteristic  $Fe^{2+}$ -CN- $Fe^{3+}$  absorption peaks. The peaks below  $1600 \text{ cm}^{-1}$  were associated with groups from the original PSF[30]. Compared with original PSF, the PSF peaks gradually shrunk as the cycle number increased. This phenomenon once again proved that controlling the cycle number successfully affected the generation of the PB layer.

### 3.3 Electrocatalytic response to glucose on PB-PSF-GOD sensor

The as-prepared membrane with embedded GOD, well dispersed PB nanoparticles combined with three dimensional porous PSF as matrix may have great potential in glucose sensor fields. As an important indicator, the activity of the PB-PSF-GOD membrane for  $H_2O_2$  catalytic reduction was evaluated. Fig. 2A shows the CVs obtained on PB-PSF-GOD and PSF-GOD membranes modified sensors for 0.4mM  $H_2O_2$  at the potential range from -0.4V to 1.2V in 0.1M PBS (pH=5). Fig. 2B displays the real and imaginary part of the EIS spectra represented as Nyquist plots for PB-PSF-GOD and PSF-GOD membranes modified sensors at frequency of 1Hz to  $10^5$  Hz using 0.1M KCl (pH=5.0) as the electrolyte. The PB-PSF-GOD has (a) larger current response, (b) lower resistance of charge transfer: the high frequency part of EIS curve of PB-PSF shows a much smaller diameter than that of PSF-GOD and (c) enhanced mass transfer: the slope of the linear part of PB-PSF-GOD EIS curve is higher than the value of PSF-GOD. The results of CV and EIS demonstrate that introducing the PB-PSF structure largely improves the catalysis for  $H_2O_2$  reduction, which means PB-PSF-GOD glucose sensors may have higher sensitivity.

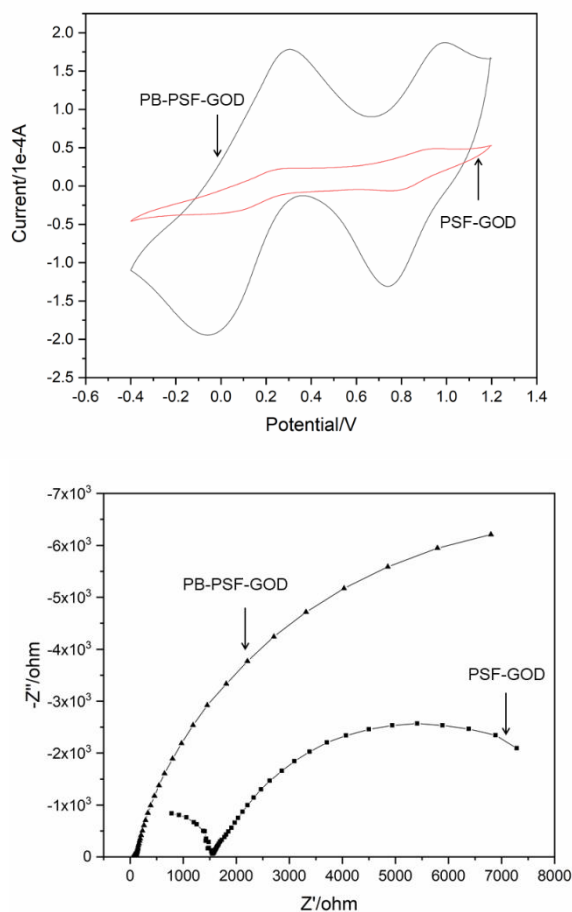


**Figure 6.** (A) CVs of 0.4mM  $H_2O_2$  on PB-PSF-GOD and PSF-GOD in 0.1M PBS (pH=5.0). Scan rate:  $0.05 \text{ Vs}^{-1}$ . (B) EIS of 0.4mM  $H_2O_2$  on PB-PSF-GOD and PSF-GOD in 0.1M KCl (pH=5.0) at frequency of 1Hz to  $10^5$  Hz.



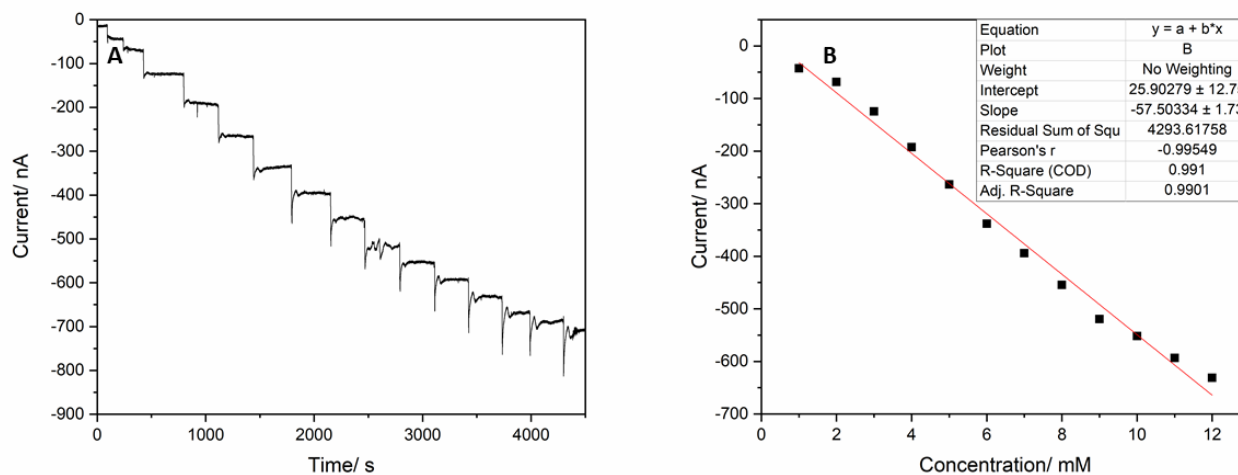


**Figure 7.** The amperometric responses of the PB-PSF-GOD biosensor to successive injection of 1 mM glucose from 0mM to 15mM in 0.05 M PBS (pH=6.5, room temperature, including 0.1 M KCl) at -0.05 V (vs. Ag/AgCl). The inset figure displays the corresponding calibration curve for glucose from 0 mM to 12 mM.

As described in 2.4, PB-PSF-GOD glucose biosensors were fabricated to evaluate its glucose analytical performance by amperometric measurements in 0.05 M PBS (pH 6.5, room temperature, including 0.1 M KCl) at an applied potential of -0.05 V (vs. Ag/AgCl) according to published study [21, 31]. The amperometric response curve for the PB covered glucose biosensor with the successive addition of glucose (1.0 mM/step) is shown in Fig. 7. Each injection was followed by stirring (200 rpm with a magnetic stirrer) for 60 s to homogenize the solution. This procedure corresponds to the sharp decline and little rebound at the beginning of each step in the curve. To verify the steady-state current for each step, each concentration was measured for 5-10 min. As the glucose concentration increased, the response current of the biosensor decreased with a linear response up to 12 mM until an obviously nonlinear current response was observed at 15 mM, which suggests saturation of the enzyme reaction. The corresponding calibration curve for the glucose response is shown in inset picture in Fig. 7. The biosensor exhibited a large linear range from 0 mM to 12 mM with a correlation coefficient of 0.991 and a sensitivity of  $0.191 \mu\text{AmM}^{-1}\text{cm}^{-2}$ . Compared with previously reported glucose biosensors (Table 1), the present biosensor extended the linear range to physiologically relevant concentration windows without a barrier layer.

As an enzyme-based biosensor, the PB-PSF-GOD glucose biosensor also followed Michaelis-Menten kinetics. The Michaelis-Menten constant,  $K_M$ , was calculated from the amperometric response curve to analyze the biosensor's glucose response behavior. The electrochemical-driven GOD catalysis Michaelis-Menten kinetics equation can be written as follows (Formula 4)[32]:

$$v = \frac{v_{\max} C_s}{C_s + K_M} \quad (4)$$

where  $K_M$  is the Michaelis-Menten constant,  $C_s$  is the glucose concentration in the solution,  $v$  is the initial velocity of the reaction and  $v_{\max}$  is the maximum reaction velocity. Using Lineweaver-Burk measurements, the value of the  $K_M$  was found to be  $0.032 \pm 0.014$  mM, which is much lower than the  $K_M$

of free GOD[33, 34] (33mM-110mM) and immobilized GOD[21] (0.44 mM). This further confirming the fewer defects, higher GOD affinity for the PB-PSF-GOD.

**Table 1.** Comparison of the performance of various PB-modified glucose biosensors.

Modifiers	Sensitivity ( $\mu\text{A mM}^{-1} \text{cm}^{-2}$ )	Linear range (mM)	Ref.
PB-PSF-GOD	7.3	1–12	This work
GOD-Chit-IL-PB-Pt	37.8	0.01–4.2	[31]
PCPB-GOD	50.63	0.1-2	[21]
GOD-MGF	2.87	1.0-12	[35]
PBA-GOD	-	0.0049-1.92	[36]
ERGO-GOD	6.82	0.02-3.2	[37]
MMC-GOD	0.513	0.5-10	[38]
RGO-AuPtNP-GOD	45	0.2-2	[39]
PEC-AuNPs-GOD	-	0.01-7	[40]
PPy-RGO-GOD	0.89	0.2-8	[41]
Nafion-AuNPs-GOD	6.5	Up to 6	[42]

Chit, chitosan; IL, ionic liquid; PC, porous carbon; MGF, Mesocellular graphene foam; PBA, Prussian blue analogue; -, not mentioned; ERGO, Electrochemically reduced GO; RGO, Reduced graphene oxide; AuPtNP, Gold and platinum alloy nanoparticle; PEC, polyelectrolyte complex; AuNPs, gold nanoparticles; PPy, polypyrrole.

The biosensor was stored in the fridge at 4°C when not in use. The stability of the biosensor was investigated by measuring the electrode response with 6 mM glucose solution every day. It was found that the biosensor retained 85% of the original response after 40 days, which indicated good stability of the biosensor.

### 3.4 Anti-interferent test

Ascorbic acid (AA) and uric acid (UA) are common GOD glucose biosensor-interfering species that always coexist with glucose in real blood samples[43]. The selectivity of the PB covered glucose biosensor was evaluated by measuring amperometric responses due to the initial addition of 0.1 mM of each interfering species and then 1.0 mM glucose followed by 0.1 mM AA and UA once again (Fig.8). A sharp glucose response was observed compared with other responses after the addition of AA and UA. This is mainly attributed to the synergistic effect of the low applied potential (−0.05 V vs. Ag/AgCl) and the PB covered structure. These results proved that the PB covered glucose biosensor had good anti-interferent abilities.

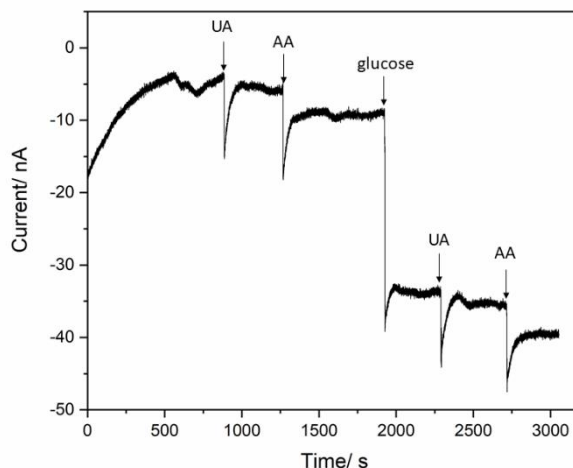


**Figure 8.** Amperometric response for 0.1mM AA, 0.1mM UA and 1.0mM glucose on the PB-PSF-GOD biosensor in 0.1 M PBS (pH=6.5, including 0.1 M KCl). Applied potential: -0.05V.

### 3.5 Human serum samples analyse

To further assess the performance of the PB-PSF-GOD glucose biosensor in blood samples, we measured glucose concentrations in fresh human serum samples after centrifuging (2000rpm, 5 min). The detected glucose concentrations in serum samples were derived from the standard curve, the regression equation and single point calibration (using one healthy volunteer serum sample). Bias values were determined by comparing glucose concentration estimated by PB-PSF-GOD glucose biosensor and YSI 2300 (Table 2). The results indicate that the PB-PSF-GOD glucose biosensor has the potential for human blood glucose determination.

**Table 2.** Analysis results in serum samples ( $N = 5$ ).

Samples No	Measured by YSI 2300 (mM)	Measured by PB-PSF-GOD glucose biosensor (mM)	%RSD	Bias (mM)
1	4.71	4.62	0.39	+0.09
2	6.02	6.09	0.12	+ 0.07
3	8.30	8.39	0.14	-0.09
4	10.15	10.31	1.55	-0.16

### 3.6 Continuous testing in serum samples

Furthermore, the longevity of the PB-PSF-GOD glucose biosensors towards the serum samples has been examined as well. The samples from one healthy volunteer and one diabetes patient were centrifuged (500rpm, 5 min) with 3% ProClin 300 as preservative. After 23 hours testing, signals decreased by about 30%, which probably due to the protein remaining in the blood enriched on the sensor. Since the second day, the glucose biosensors only attenuated no more than 10% after 7 days

continuous testing (Table 3). The results indicate that PB-PSF-GOD glucose biosensor has potential applications in CGM.

**Table 3.** Continuous testing results in serum samples.

Time (h)	1	24	48	72	96	120	144	168	192
Sample 1	-345	-240	-242	-239	-238	-235	-232	-230	-228
Sample 2	-565	-397	-396	-395	-394	-384	-382	-380	-370

#### 4. CONCLUSIONS

In conclusion, a novel PB-PSF stereo-structure with interlocked GOD was fabricated, and a good performance glucose biosensor was developed based on this structure. With GOD interlocked in the porous hydrophilic modified PSF membranes, a self-assembled PB layer was formed around the substrate. Fifteen reactions cycles were proven to be the optimal procedure forming well-dispersed PB layer. The experiments revealed that the PB-PSF-GOD glucose biosensor had large linear range, high affinity, good selectivity and long sensor life. The PB-PSF-GOD glucose biosensor may have promising applications in enzymatic biosensors, especially the CGM.

#### SUPPORTING MATERIAL:

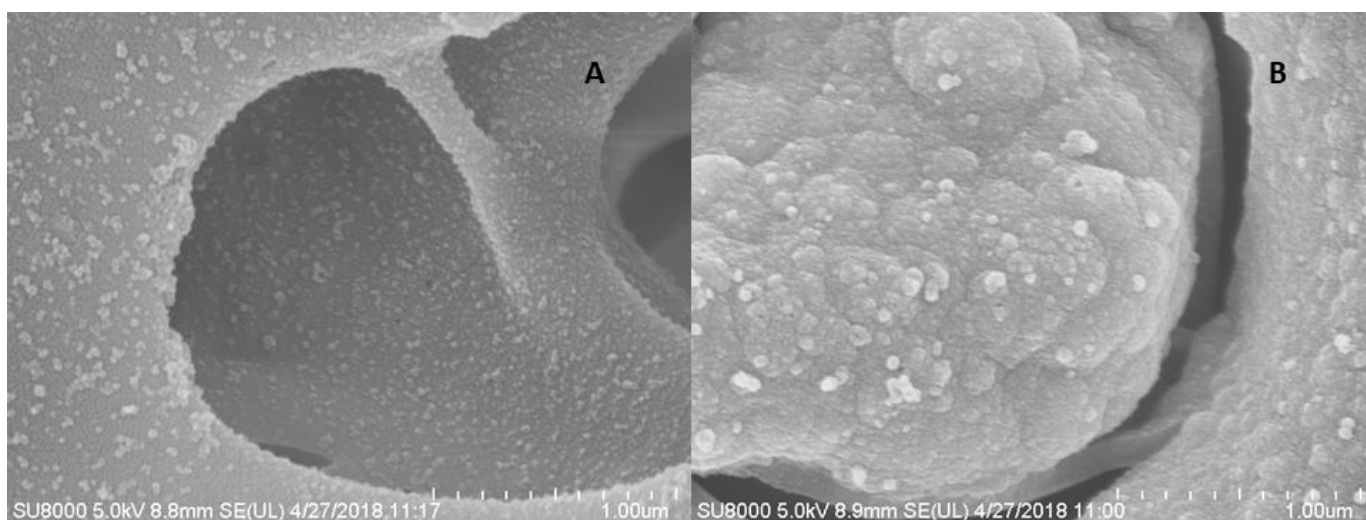


**Figure S1.** SEM images of PB-PSF-GOD prepared with 0.1 M glucose solution mixture(a) and 1M glucose solution mixture(b)

## ACKNOWLEDGMENTS

This research was supported by the Zhejiang Provincial Natural Science Foundation of China (Grant No. LY18H180009) and the Zhejiang Province Key R&D Project (Grant No. 2017C03029).

## References

1. B. Guerci, M. Floriot, P. Böhme, D. Durain, M. Benichou, S. Jellimann and P. Drouin, *Diabetes care*, 26 (2003) 582.
2. P. Schaepelynck-Belicar, P. Vague, G. Simonin and V. Lassmann-Vague, *Diabetes & metabolism*, 29 (2003) 608.
3. M. C. Moreno-Bondi, O. S. Wolfbeis, M. J. Leiner and B. P. Schaffar, *J. Anal. Chem.*, 62 (1990) 2377.
4. J. Wang, *Chemical reviews*, 108 (2008) 814.
5. D. Olczuk and R. Priefer, *Diabetes Metab Syndr*, 12 (2018) 181.
6. Y. Luo and Y. Bao, P. Zhang, D. Zhu, X. Li, J. Ji, H. Zhang and L. Ji, *Diabetes Technology&Therapeutics*, 19(2017)13.
7. I. Lee, N. Loew, W. Tsugawa, C.E. Lin, D. Probst, J. T. La Belle and K. Sode, *Bioelectrochemistry*, 121 (2018) 1.
8. Z. Chu, Y. Liu and W. Jin, *J. Biosens. Bioelectron.*, 96 (2017) 17.
9. K. Itaya, I. Uchida and V. D. Neff, *J. Acc. Chem. Res.*, 19 (1986) 162.
10. B. Kong, C. Selomulya, G. Zheng and D. Zhao, *Chemical Society Reviews*, 44 (2015) 7997.
11. T. Yamamoto, N. Saso, Y. Umemura and Y. Einaga, *J. Am. Chem. Soc.*, 131 (2009) 13196.
12. A. A. Karyakin, E. E. Karyakina and L. Gorton, *J. Anal. Chem.*, 72 (2000) 1720.
13. P. Yang, J. Peng, Z. Chu, D. Jiang and W. Jin, *J. Biosens. Bioelectron.*, 92 (2017) 709.
14. Y. Zhang, B. Huang, F. Yu, Q. Yuan, M. Gu, J. Ji and Y. Zhang, Y. Li, *Microchimica Acta*, 185 (2018) 86.
15. L. Wang, S. Tricard, P. Yue, J. Zhao, J. Fang and W. Shen, *J. Biosens. Bioelectron.*, 77 (2016) 1112.
16. M. A. Komkova, E. E. Karyakina and A. A. Karyakin, *J. Anal. Chem.*, 89 (2017) 6290.
17. D. Feng, X. Lu, X. Dong, Y. Ling and Y. Zhang, *Microchimica Acta*, 180 (2013) 767.
18. X.J. Zheng, Q. Kuang, T. Xu, Z.Y. Jiang, S.H. Zhang, Z.X. Xie and R.B. Huang, *The Journal of Physical Chemistry C*, 111 (2007) 4499.
19. X. Mu, T. Bertron, C. Dunn, H. Qiao, J. Wu, Z. Zhao and C. Saldana, H.J. Qi, *Materials Horizons*, 3 (2017) 442.
20. M. Yang, Y. Liu, Y. Song, G. Zhao, H. Tan, Q. Zhang and F.G. Xu, *Int. J. Electrochem. Sci*, 12 (2017) 4428.
21. B. Thakur, X. Guo, J. Chang, M. Kron and J. Chen, *Sensing and Bio-Sensing Research*, 14 (2017), 47.
22. S. Cinti, R. Cusenza, D. Moscone and F. Arduini, *Talanta*, 187 (2018) 59.
23. E. L. G. Medeiros, A. L. Braz, I. J. Porto, A. Menner, A. Bismarck, A. R. Boccaccini, W.C. Lepry, S.N. Nazhat, E.S. Medeiros and J.J. Blaker, *J. ACS Biomate. Sci. Eng.*, 2 (2016) 1442.
24. P. A. Fiorito, V. R. Gonçalves, E. A. Ponzio and S. I. C. de Torresi, *J. Chem. Commun.*, (2005) 366.
25. W. Zhang, L. Wang, N. Zhang, G. Wang and B. Fang, *Electroanalysis*, 21 (2009) 2325.
26. Y. Xu, Z. Chu, L. Shi, J. Peng and W. Jin, *Sensors and Actuators B: Chemical*, 221 (2015) 1009.
27. Y. Cheng, J. Tao, G. Zhu, J. A. Soltis, B. A. Legg, E. Nakouzi, J. Deyoreo, M.L. Sushko and J. Liu, *Nanoscale*, 10 (2018) 11907.
28. M. Planche, J. Thieblemont, N. Mazars and G. Bidan, *Journal of Applied Polymer Science*, 52

- (1994) 1867.
29. P. K. Lee, P. M. Nia and P. M. Woi, *Electrochimica Acta*, 246 (2017) 841.
  30. T. Huang, M. Zhang, L. Cheng, L. Zhang, M. Huang, Q. Xu and H. Chen, *RSC Advances*, 3 (2013) 25982.
  31. Y. Zhang, Y. Liu, Z. Chu, L. Shi and W. Jin, *Sensors and Actuators B: Chemical*, 176 (2013) 978.
  32. S. Krishnan, J. B. Schenkman and J. F. Rusling, *J. Biol. chem.*, 115 (2011) 8371.
  33. Q. H. Gibson, B. E. Swoboda and V. Massey, *J. Biol. chem.*, 239 (1964) 3927.
  34. B. E. Swoboda and V. Massey, *J. Biol. chem.*, 240 (1965) 5.
  35. H. Li, Y. Wang, D. Ye, J. Luo, B. Su, S. Zhang and J.L. Kong, *Talanta*, 127 (2014) 255.
  36. Y. Song, J. He, H. Wu, X. Li, J. Yu, Y. Zhang and L. Wang, *Electrochimica Acta*, 182 (2015) 165.
  37. L. Liu, Y. Gou, X. Gao, P. Zhang, W. Chen, S. Feng and Y.D. Li, *Materials Science and Engineering: C*, 42 (2014) 227.
  38. A. H. Valekar, B. S. Batule, M. I. Kim, K.H. Cho, D.Y. Hong, U.H. Lee, J.S. Chang, H.G. Park and K.Y. Hwang, *J. Biosens. Bioelectron.*, 100 (2018) 161.
  39. X. Xuan, H. S. Yoon and J. Y. Park, *J. Biosens. Bioelectron.*, 109 (2018) 75.
  40. I. Rassas, M. Braiek, A. Bonhomme, F. Bessueille, G. Raffin, H. Majdoub and N.R. Jaffrezic, *Sensors*, 19 (2019) 154.
  41. B. Wu, S. Hou, Y. Xue and Z. Chen, *Nanomaterials*, 8 (2018) 993.
  42. S. Zhao, K. Zhang, Y. Bai, W. Yang and C. Sun, *Bioelectrochemistry*, 69 (2006) 158.
  43. S. Husmann, E. Nossol and A. J. G. Zarbin, *Sensors and Actuators B: Chemical*, 192 (2014) 782.